ELSEVIER

Journal of Structural Geology 27 (2005) 2113–2134

JOURNAL OF STRUCTURAL GEOLOGY

www.elsevier.com/locate/jsg

Basin inversion by distributed deformation: the southern margin of the Bristol Channel Basin, England

R.A. Glen*, P.L. Hancock[b,✠], A. Whittaker[c]

[a]*Geological Survey of New South Wales, Department of Primary Industries, Box 344, Hunter Regional Mail Centre, New South Wales 2310, Australia*
[b]*Department of Geology, University of Bristol, Wills Memorial Building, Queens Road, Bristol BS8 1RJ, UK*
[c]*British Geological Survey, Keyworth, Nottinghamshire NG12 5GG, UK*

Received 14 June 2005; accepted 1 August 2005
Available online 2 November 2005

Abstract

Several models of basin inversion described in the literature are tested in a study of Triassic and Early Jurassic strata exposed along the southern margin of the Bristol Channel Basin in Somerset, England that has been exhumed by <3 km. Two key features of the superbly exposed normal faults are that they formed at several times during basin evolution—not during Triassic to Early Jurassic growth, but during Late Jurassic rifting, and during and after inversion; and that $>95\%$ of them are still in net extension, despite widespread kinematic evidence for reverse reactivation. When coupled with the general absence of thin-skinned thrusts and the widespread occurrence of regional contractional folds, it appears that none of three main inversion models—the fault-reactivation model, the thin-skinned model and the buttress model—are by themselves applicable. We erect a new model of basin inversion, the distributed deformation model, which consists of three stages of basin inversion. Stage one involved early partial reactivation of large-displacement steep normal faults. Stage two was dominated by folding, wherein fault blocks underwent oblique (non-coaxial) shortening by map scale folding, accompanied by formation of outer arc normal faults, minor cleavage and neoformed thrusts. Stage three involved reverse reactivation of outer arc normal faults and activation of oblique and strike-slip faults that partitioned deformation into compartments.

Keywords: Bristol Channel Basin; Extensional faulting; Basin inversion; Folding; Distributed deformation

1. Introduction

The deformation and extrusion of all or part of the fill of an extensional sedimentary basin is called basin inversion (Cooper and Williams, 1989a,b; Buchanan and Buchanan, 1995). Several models of inversion have been postulated:

(1) *Fault-reactivation model*. In this, the most popular model, basin inversion takes place by the progressive, top-to-bottom reverse reactivation of extensional growth faults (with formation of derivative splay and shortcut structures), so that the null or changeover point (from contraction above to extension below) moves down the fault surface (papers in Cooper and Williams, 1989a,b; Buchanan and Buchanan, 1995). Reactivation is generally selective, with the shallowest dipping faults reactivating preferentially unless fluid pressure reduces cohesion on steeper faults (Coward, 1994; Sibson, 1995). This model is supported from seismic studies in submarine basins (Badley et al., 1989), field studies of fold and fault geometries in more strongly inverted basins that occur in orogenic belts (de Graciansky et al., 1989; McClay et al., 1989) and analogue studies (McClay, 1995).

(2) *Thin-skinned model*. In this model, extensional faults, because of orientation, buttressing or other reasons, undergo only minor reactivation or are not reactivated. Shortening of basin-fill is accomplished by formation of neo-formed, thin-skinned thrusts. Support for this model comes principally from inverted basins in the external parts of orogenic belts (Gillcrist et al., 1987; Powell, 1987; Welbon, 1988; Butler, 1989; Bishop and Buchanan, 1995). Similar relations have been recorded in some sandbox models (McClay, 1989).

* Corresponding author.
E-mail address: dick.glen@dpi.nsw.gov.au (R.A. Glen).
✠ Deceased.

0191-8141/$ - see front matter © 2005 Elsevier Ltd. All rights reserved.
doi:10.1016/j.jsg.2005.08.006

(3) *Buttress model*. In this model, basement rocks in the footwalls of older steep normal faults form mechanical barriers to the contractional reactivation of normal faults and to thin-skinned thrusting along or near the basement-cover interface. As a result, shortening of basin-fill by folding and back-thrusting is concentrated in the hanging walls of early extensional faults, and may be accompanied by the minor reverse reactivation of the upper parts of those faults. Field examples have been described by several authors (Gillchrist et al., 1987; Welbon, 1988; Butler, 1989; Sibson, 1995).

Complexity is added to these models when the directions of opening and closing are not parallel, leading to oblique or

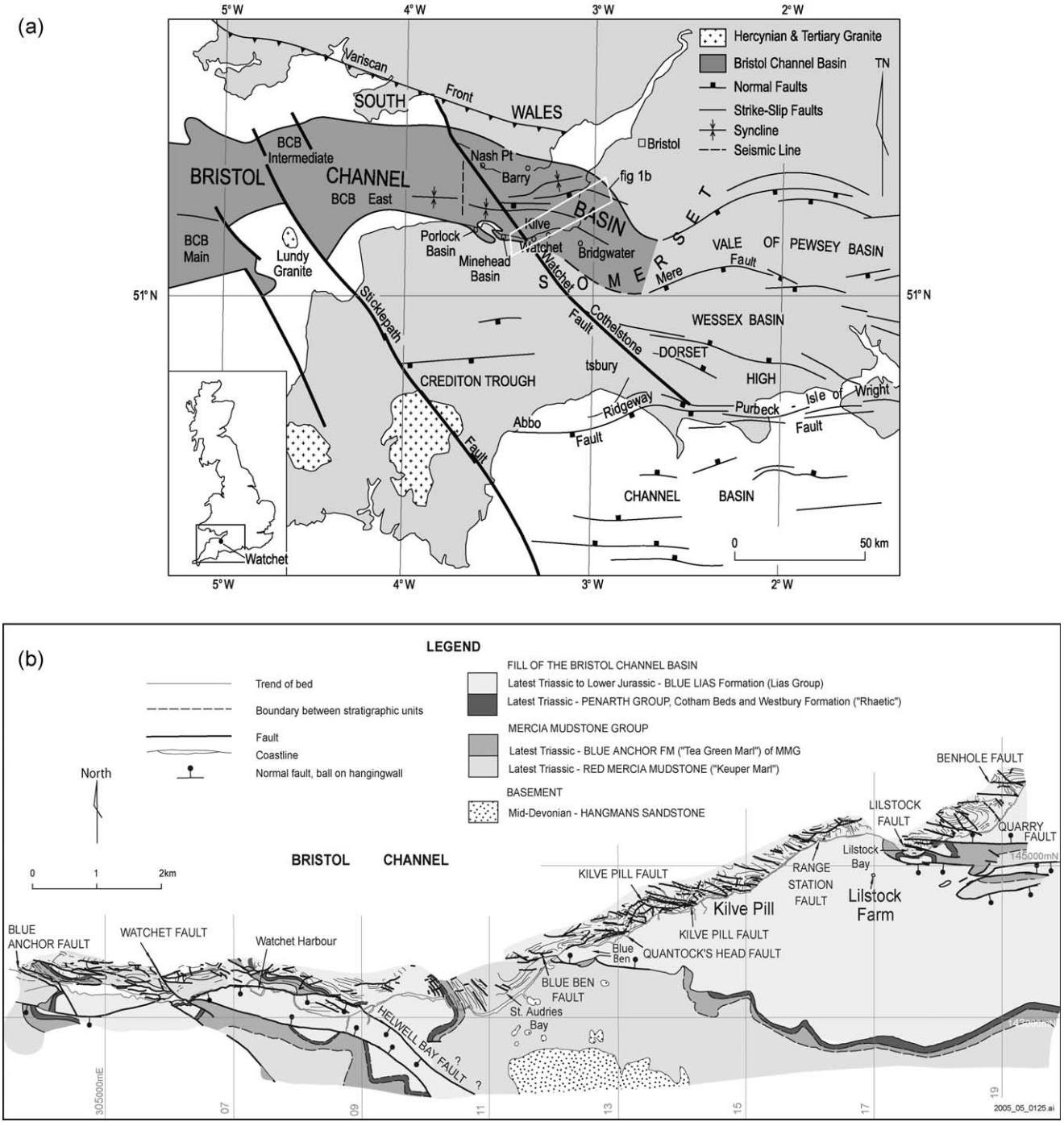

Fig. 1. (a) Location map showing the Bristol Channel Basin in relation to surrounding basins in southwest England. The Watchet–Cothelstone fault is after Whittaker (1972), with extension to Nash Point in Wales after Owen (1971). Modified from Dart et al. (1995), Lake and Karner (1987) and van Hoorn (1987). (b) Synthesis of the structure of the southern margin of the Bristol Channel Basin. Inland geology based on compilation of the Weston-super-Mare, Taunton and Minehead 1:50,000 scale maps of the British Geological Survey. The Porlock and Minehead basins are two north-facing half grabens (Whittaker, 1976; Edwards, 1999) separated by a basement horst from the main basin offshore. Coastline geology from this study.

transpressional closing of extensional basins (Lowell, 1995; Turner and Williams, 2004). Oblique deformation may be taken up by the formation of neoformed inversion structures that are not coaxial with extensional structures, or by the strike-slip or oblique-slip reactivation of extensional structures (Harvey and Stewart, 1998). In a three-dimensional strain field, these oblique faults act to partition inversion into compartments with different structural styles. Cartwright (1989) pointed out reactivation of basement cross-structures could also produce segmentation of inversion structures.

In order to investigate the possible linkages between extensional and contractional structures, and thus how basins begin to invert, we carried out a study of the southern margin of the Bristol Channel Basin in southwest England (Fig. 1a and b)—a margin now preserved just above sea level and which has close to 100% outcrop on wide rock platforms and superb cliff sections. The nature of this outcrop is so good that it has previously attracted several unpublished field guides (Hancock, 1985; McClay and Dart, 1993; Davison, 1994) and has become a type area for studies in basin formation and inversion (Whittaker, 1975; Dart et al., 1995; Nemčok et al., 1995), normal faulting (Peacock and Sanderson, 1991), strike-slip faulting (Peacock and Sanderson, 1996), and jointing (Rawnsley et al., 1998; Engelder and Peacock, 2001).

Very early in our study three key things became apparent: (i) there was little evidence for syndepositional normal faulting; (ii) virtually all of the normal faults were still in net extension, despite the exhumation of the basin margin and the kinematic evidence for reverse reactivation; and (iii) there was kinematic evidence that some extensional faults had undergone oblique to strike-slip reactivation, so that basin closing was not coaxial with basin opening.

So in an attempt to understand how the southern margin of the Bristol Channel Basin was uplifted, we adopted a two-stage approach. In addition to a detailed examination of outcrop-scale structures, we produced a detailed structural map of the basin margin, whereby we could assess the role played by individual outcrop-scale structures in relation to larger map-scale features and thus to the overall exhumation of the basin.

To do this, we used ~1:500 scale annotated aerial photographs used by A.W. for his detailed biostratigraphic mapping, which up to now has been only partly published (Whittaker et al., 1980; Whittaker and Green, 1983). These photos became the base for our new map of the basin margin, extending from Blue Anchor in the west to Benhole Point (west of Hinkley Point) in the east (Fig. 1b). The eastern 10 km of the basin margin west of Benhole Point (Fig. 1b) were structurally re-mapped at a scale of 1:7500. The western 7 km of the basin margin, from St Audries Bay through Watchet to Blue Anchor (Fig. 1b), were more briefly examined, with this part of the map (at a scale of 1:17,000) based on reconnaissance structural observations superimposed on A.W.'s original mapping.

2. Regional geological setting and basin fill

The Bristol Channel Basin is a largely Mesozoic basin between Wales and Somerset. It is segmented into three parts by NW-trending strike-slip faults (Fig. 1a) (Kamerling, 1979; Whittaker and Green, 1983; Brooks et al., 1988). The eastern part (henceforth referred to as the Bristol

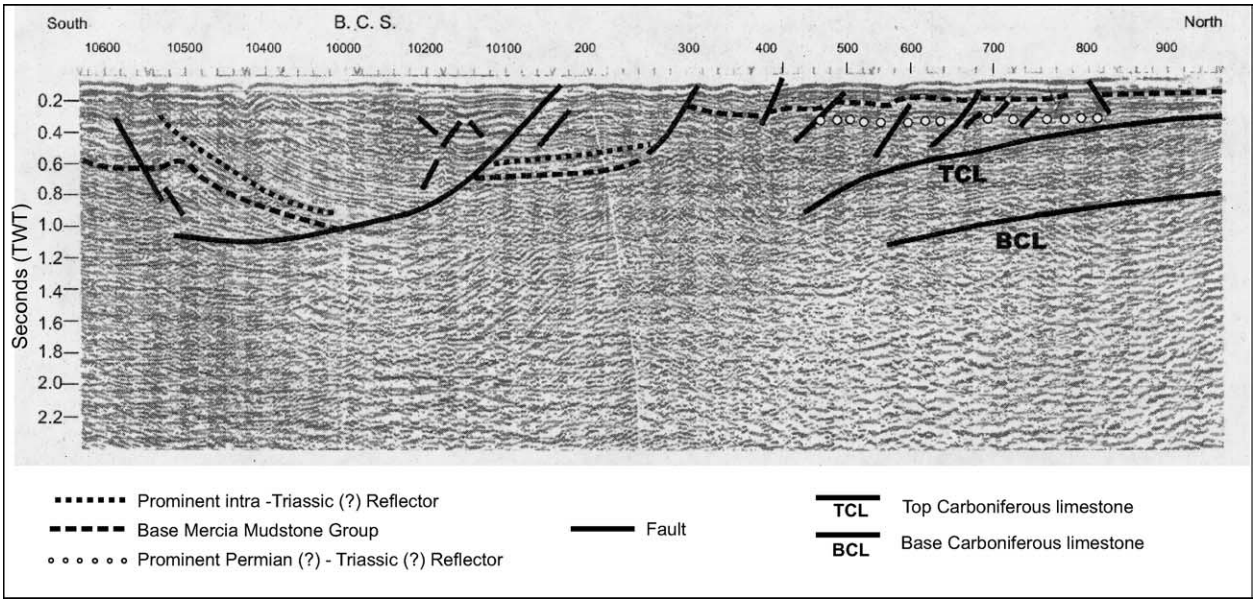

Fig. 3. Interpretation of north–south seismic line across the Bristol Channel Basin (dashed line in Fig. 1a), based on seismic data courtesy of Geco-Prakla (UK). The northern part of this line was published by Brooks et al. (1988). B.C.S. = Bristol Channel Syncline.

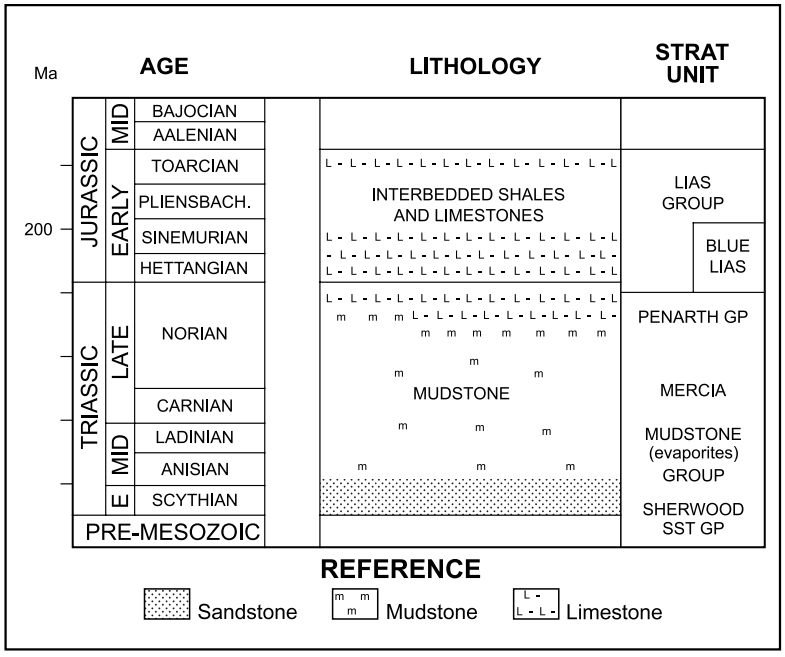

Fig. 4. Summary stratigraphic table for Triassic and Jurassic strata of the Bristol Channel Basin. Based largely on Kamerling (1979) and Tappin et al. (1994).

Channel Basin) outcrops on land and passes eastward via the Central Somerset Basin (Whittaker, 1975) into the Vale of Pewsey Basin (Lake and Karner, 1987; van Hoorn, 1987) (Fig. 1a). Basement consists of Devonian Old Red Sandstone and Carboniferous limestone. East of Minehead in Somerset, the basin/basement contact has been interpreted as either faulted (Owen, 1971) or unconformable (Tappin et al., 1994).

Table 1
Details of Triassic and Jurassic stratigraphy based on Whittaker (unpublished mapping), Whittaker and Green (1983) and Tappin et al. (1994)

Jurassic to basal Triassic	Lias Group	Blue Lias Formation (275 m thick). Open marine limestones and interbedded shales and marls, divided into five divisions that correspond with biostratigraphic units defined by ammonite species. (Whittaker (unpublished mapping) and Whittaker and Green (1983))	Cz (1 locality only)	Shale/limestone ratio of 10.8:1
			Bz (40 m thick)	Shales and limestones interbedded in the ratio 6.9–8.8:1
			Az (50 m thick)	Shales and limestones in the ratio 2.5–5.6:1
			Lz (25 m thick)	Fissile and incompetent shales with a shale/limestone ratio of 12.8–13.7:1—least competent
			Pz (17.5 m thick)	Shales and limestones interbedded in the ratio 1.9–3.5:1—the most competent
Triassic	Penarth Group	Lilstock Formation (4 m thick)		Mudstone passing up into interbedded limestones and shales; more competent than Westbury Formation
		Westbury Formation (13 m thick)		Mudstone
	Mercia Mudstone Group (Kamerling, 1979; Whittaker and Green, 1983; Tappin et al., 1994; Edwards, 1999)	Blue Anchor Formation (unit TGM, 'Tea Green Marl')		Gypsum-rich bedded mudstones, siltstones and marls. More mechanically competent and displays small fault arrays in several locations
		Lower red Mercia Mudstone (unit Km or 'Keuper Marl')		Marl with gypsum-veined evaporite horizons. Relatively weak unit, although able to sustain hydraulic fracturing in response to elevated fluid pressures (Cosgrove, 2001)

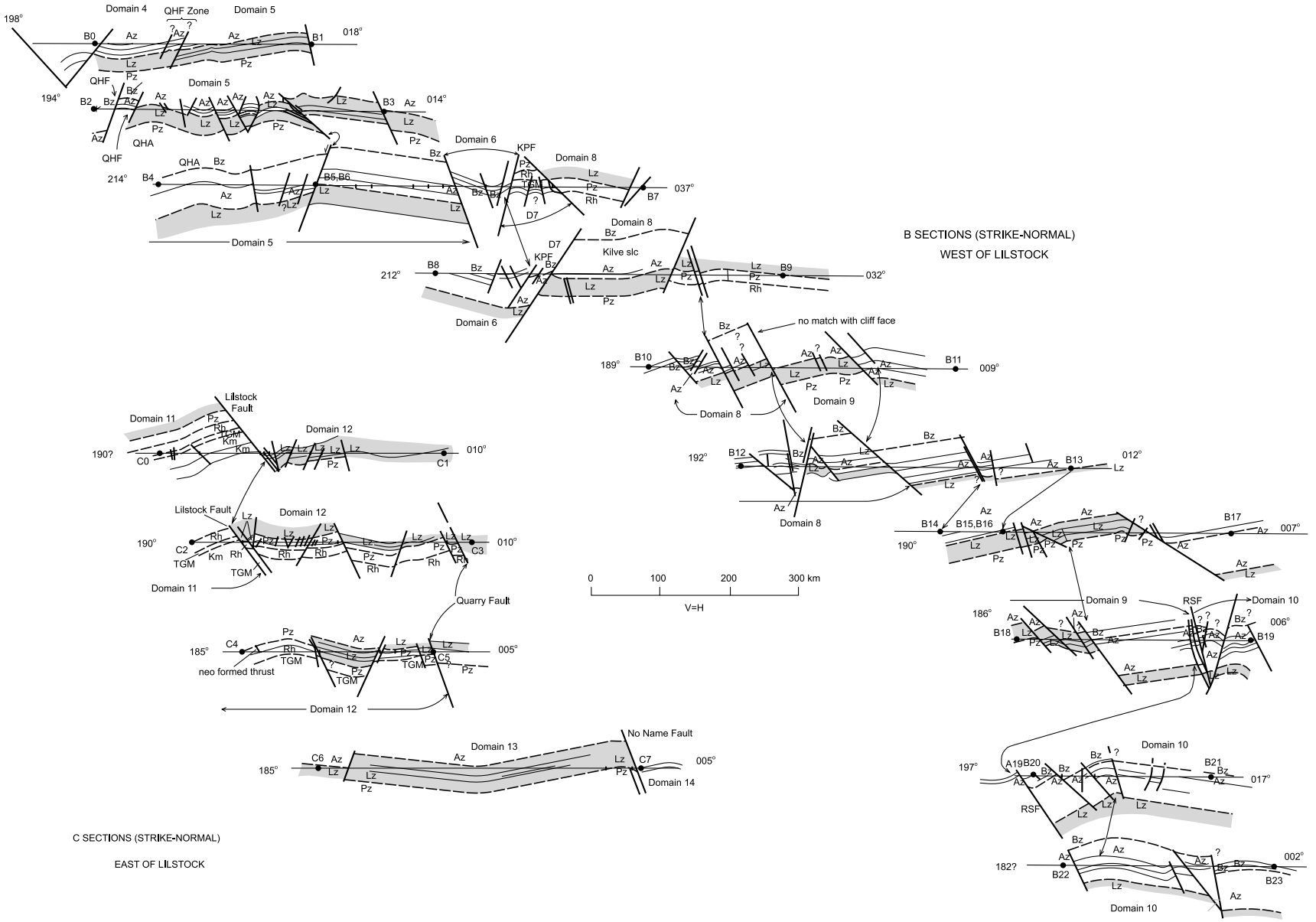

Fig. 5. Profile cross-sections, B0–B23 west of Lilstock and C0–C7 east of Lilstock constructed along rock platform. Note the considerable variation in fold geometry.

The Bristol Channel Basin is asymmetrical. Faulted subhorizontal strata in the northern margin in Wales (Nemčok et al., 1995) extend offshore and are cut by down-to-the-south normal faults (Fig. 3) (Brooks et al., 1988). The central part of the basin is filled by basal Jurassic and younger strata in a (?half) graben, subsequently deformed into the regional Bristol Channel Syncline and flanked to the north by the south-dipping central Bristol Channel Basin Fault Zone (Figs. 1a and 3) (Lloyd et al., 1973; Kamerling, 1979; Brooks et al., 1988). The southern margin, the subject of this paper, is more strongly deformed into large wavelength open folds cut by mainly east–west and WNW-trending faults (Figs. 1b and 2a (see accompanying CDRom or the on-line version of this article for Fig. 2) that also extend offshore (Fig. 3; see also Dart et al., 1995).

The Bristol Channel Basin contains Permian to Oligocene strata (Kamerling, 1979; van Hoorn, 1987; Brooks et al., 1988; Tappin et al., 1994; Edwards, 1999). Triassic–Early Jurassic sedimentary rocks outcrop on the southern margin and are largely marly and muddy. Younger strata are recorded from drill cores and seismic lines in the Bristol Channel, and reflect Middle and Late Jurassic extension followed by thermal relaxation. They are overlain by scattered Cretaceous and Tertiary strata (Tappin et al., 1994).

Along the southern margin, Triassic evaporites and mudstones represent initial rift subsidence. They belong to the Triassic Mercia Mudstone Group (Fig. 4). The following sag phase resulted in deposition of lower Jurassic limestones in open shallow marine conditions—the Penarth Group and Blue Lias Formation of the Lias Group (Fig. 4) (Tappin et al., 1994) (Table 1).

Strata along the southern margin are largely marly or muddy; only the limestone beds impart structural rigidity, and their presence influences the spacing of small fractures, the tightness of folds, and intensity of fracturing. The most competent unit Pz has the highest limestone:shale ratio (Table 1) and displays open folds that are controlled by thick, dominant limestone beds that are commonly cut by fractures. In the least competent unit Lz, fold hinges are much less fractured, tighter, and of smaller wavelength.

Exhumation of the Bristol Channel Basin seems to have been a multistage process. From stratigraphic evidence, Kamerling (1979) and Tappin et al. (1994) suggested that the main exhumation occurred in the Early Cretaceous, with lesser, intermittent activity in the Tertiary. Strontium isotope data from a carbonate fault seal indicated probable Oligocene exhumation (Hunsdale et al., 1995). The suggestion of widespread Tertiary exhumation in southwest England, driven either by magmatic underplating (Brodie and White, 1994) or decoupled lithospheric compression (Hillis, 1992), raises the question of how much the exhumation of the Bristol Channel Basin was driven by localised upper crustal compression leading to structural inversion, and how much by regional lithospheric processes. Menpes and Hillis (1995) suggested ~1 km of regional Tertiary exhumation. This is approximately half of the 2.4–3 km of exhumation estimated by Cornford (1986) from vitrinite reflectance measurements. More recently, Holford et al. (2005) used fission track data to suggest the Bristol Channel Basin had undergone up to 3 km of exhumation in the Cretaceous, limited early Palaeogene exhumation and ~1 km of exhumation in the Late Palaeogene–Neogene.

3. Structures

The fold and fault geometry of the southern margin of the Bristol Channel Basin is shown in plan view in Fig. 2a, in a cliff line section that varies from profile to oblique view in Fig. 2b and in overlapping profile sections in Fig. 5.

On a regional scale, the most obvious feature is a central horst occupied by the Mercia Mudstone Group and separated from younger rocks by outwardly dipping faults (Fig. 1b). A smaller horst in the east of the study area is cut by internal faults. Small horsts and grabens in the west of the area are cut by the NW-trending Watchet Fault, a reverse strike-slip fault (Whittaker, 1972). A graben east of that fault is bounded to the north by the Helwell Bay Fault. Relations are more complex west of the Watchet Fault (Fig. 1b).

Table 2
Features of non-planar extensional faults

Bedding parallel faults	Zones rich in gypsum veins in red Mercia Mudstone = stratigraphic seals (Davison, 1994) or permeability barriers (Dart et al., 1995). Shale rich units in TGM (Fig. 6a). Fibred calcite veinlets that form parts of linked arrays in Blue Lias (Fig. 6b) (cf. Dart et al., 1995)
Listric and ramp-flat faults	Includes true listric faults in both the Liassic and older units (Fig. 6a), as well as ramp-flat faults. Anticlines developed in some hanging walls may reflect accommodation of bedding to non-planar extension on listric normal faults
Ductile–brittle extensional shear zones	Type (i): incoherent with complexly folded and internally faulted zones and poorly defined edges. Type (ii): well-defined boundaries, defined by the crests of hanging wall anticlines and footwall synclines, or by younger discrete faults. Bedding within zones dips steeply (up to 52°) in the same direction as the shear zone boundaries (Fig. 6c), thus helping to define shear zone dip on rock platforms. Type (iii): extreme example of normal-sense fault 'drag' with marked attenuation of rotated bedding in shear zone, the removal of shale interbeds, flow of shale into dilatant sites and juxtaposition of parts of different limestone beds separated by discontinuities, discrete faults or thin shale films

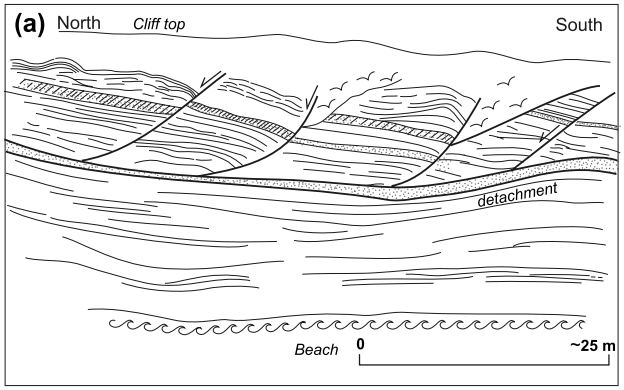

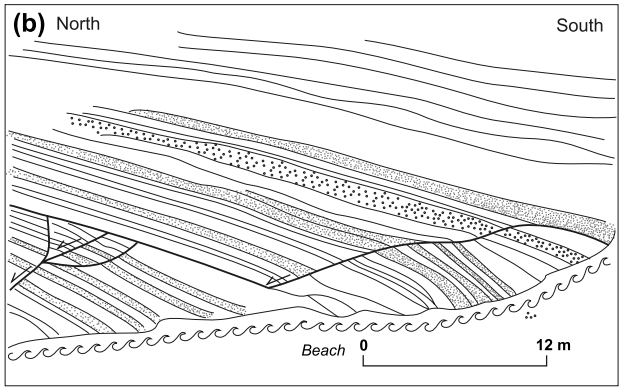

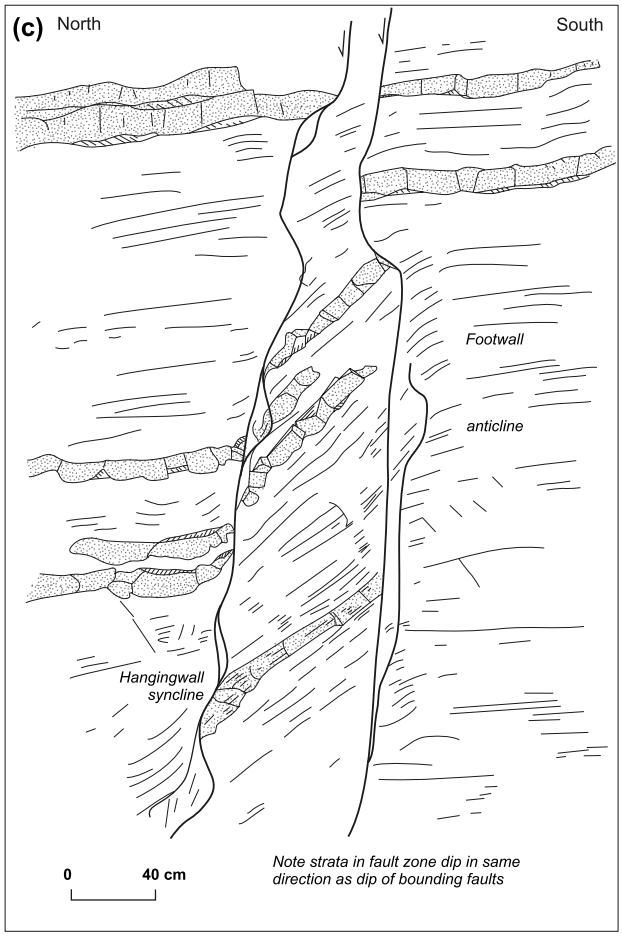

Fig. 6. Sketches of normal faults. (a) Listric faults in the Penarth Formation soling onto high-level detachment in Blue Anchor Formation (TGM). Domain 11. (b) Extensional fault system consisting of bedding parallel detachments, marked by calcite veinlets, linked into early planar normal faults rotated into gentle dips in south limb of Range Station Anticline. Domain 10. Unit Az. (c) Normal sense shear zone showing localised hanging wall syncline and footwall anticline. Rotated bedding within the shear zone dips in the same direction as throw. Unit Lz, domain 13.

Within Liassic rocks, the most obvious map-scale features are regional WNW-trending folds and parallel faults (Figs. 1b and 2a). Using differences in geometry summarised in the Appendix (see accompanying CDRom or the on-line version of this article), the basin margin has been divided into 14 domains that are bounded by partially reactivated, major normal faults. Regional folds dominate all domains except domain 9 (Fig. 2a), but even here there are some fold pairs.

Here we briefly summarise the different types of structures. Details are in the Appendix.

3.1. Structures formed by north–south extension

- Mesoscopic extensional faults and folds are the most common structures.
- Extensional faults show normal stratigraphic separation of bedding and extensional kinematics on the fault surface such as normal-sense striae, fibres and tool marks (cf. Petit, 1987; Angelier, 1994).
- Fault morphology varies from barren cracks to calcite or gypsum-veined structures up to several cm thick consisting of polished laminated vein and wallrock layers (e.g. Davison, 1995).
- Planar normal faults dominate. Many show evidence of contractional reactivation as discussed below.
- Bedding-parallel faults, listric and ramp-flat faults and extensional shear zones (Table 2) are less common (Fig. 6a – c).

3.1.1. Planar normal faults

Planar normal faults have the following characteristics:

- General ~east – west strikes and near dip-slip kinematics (Figs. 2a, blue arrows and 7a – c). At map scale, many faults are curved or branch.
- Dips between 35 and 80°, but anywhere from <5 to $>90°$ (i.e. overturned) in mudstone (Fig. 8a – c). Faults may be 'refracted' in some limestone beds, with formation of local extensional duplexes (Whittaker and Green, 1983; Peacock and Sanderson; 1991; McGrath and Davison, 1995).
- Dips largely independent of bedding dips, although faults with dips $<20°$ occur where bedding dips are $>20°$ (Fig. 8d).
- Displacements <2 m, too small to be normally imaged by

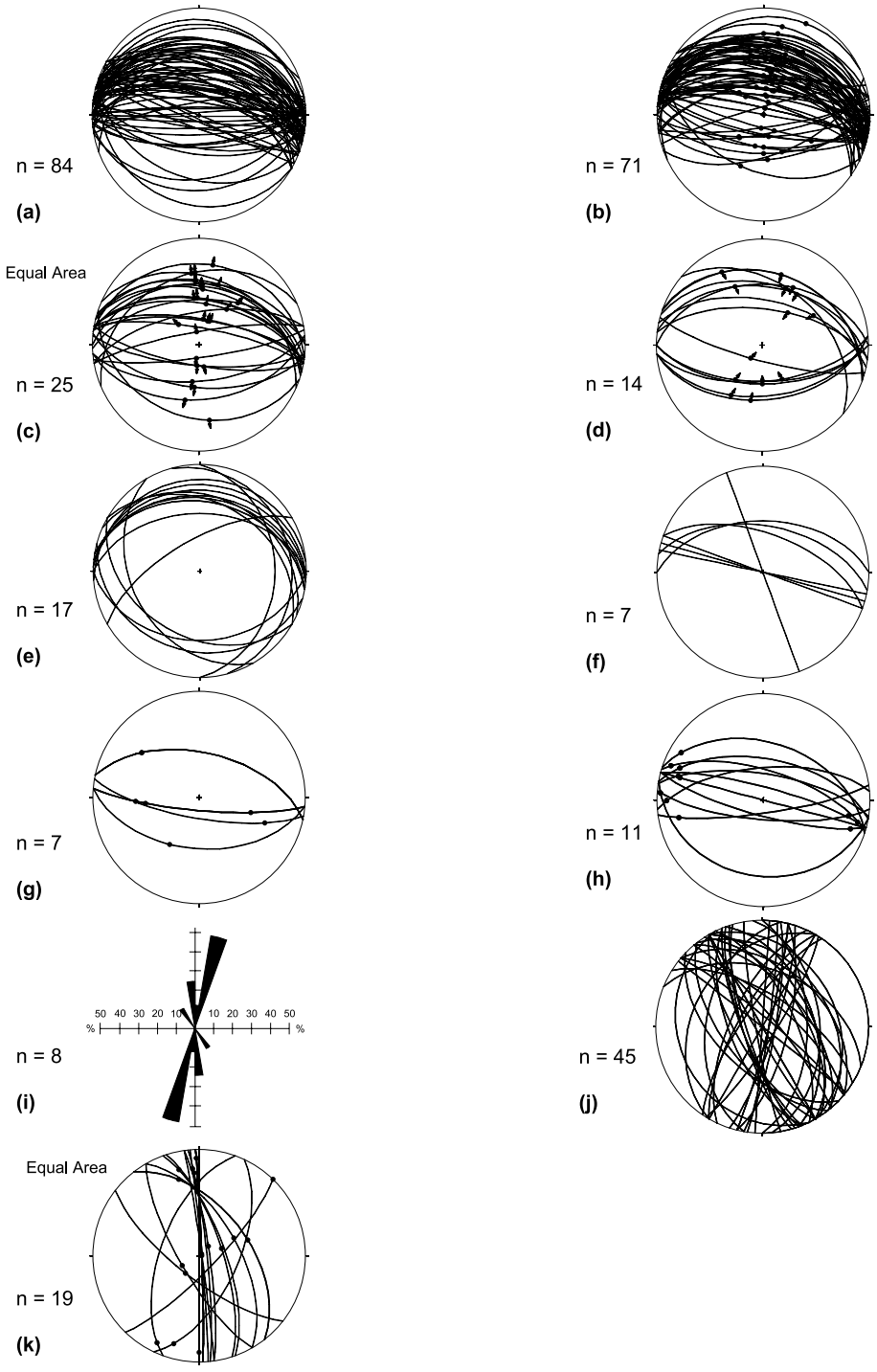

Fig. 7. Orientation data, equal area, lower hemisphere plots where appropriate, with number of data points in lower left of each figure. (a) Steep normal faults. Note dominance of northward, basinward dips and the more north-westerly faults of domain 3. (b) Steep planar normal faults with slickenfibres of uncertain sense. (c) Steep normal faults with slickenfibres of normal sense. (d) Steep normal faults with reverse-sense slickenfibres. (e) Neoformed thrusts. (f) Cleavage. (g) Steep normal faults with oblique-sense slickenfibres. (h) Steep normal faults with strike-sense slickenfibres. (i) Rose diagram of deformed ammonites. (j) Cross faults, consisting of a set of NE-trending faults and a set of N-NW-trending faults. (k) Cross faults showing largely strike-slip lineations on NE-trending set and strike and dip slip lineations on N-NW-trending set. Data plots were produced using program FaultKinWin by Allmendinger (2001), Stereonet for Windows by Allmendinger (2002) and GEOrient from Rod Holcombe.

seismic reflection profiling, but range up to 220 m (Fig. 8a and b). The largest faults throw the Blue Lias (or Blue Anchor Formation) in the hanging wall down against the red Mercia Mudstone in the footwall. They include the Lilstock Fault (domain 11, 76 m displacement), Blue Anchor Fault (~80 m), Helwell Bay Fault (domain 2, ~210 m) and the Blue Ben Fault (domain 3, ~220 m) (Fig. 9). In contrast, the No Name Fault, (domain 13,

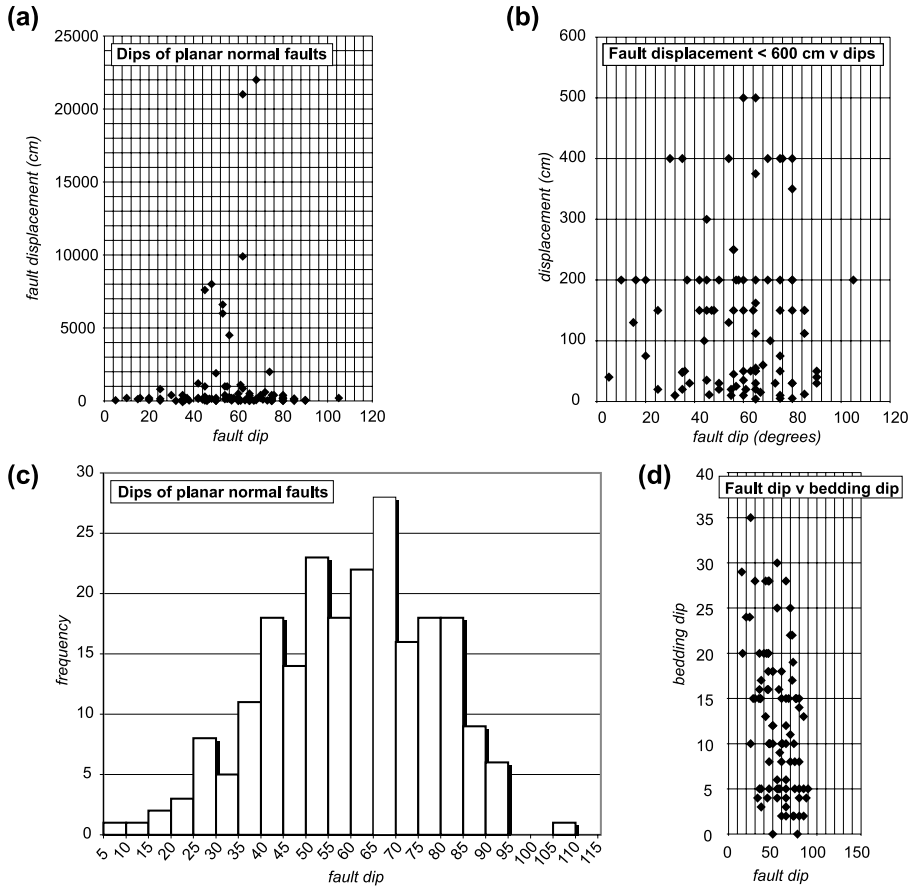

Fig. 8. Dip data of planar normal faults with unambiguous extensional kinematics. Only dips in shale beds are recorded where significant refraction occurs in limestone beds. (a) Plot of fault dip against fault displacement, showing the wide range of fault dips and subdivision into displacement groups discussed in the text. (b) Detail of (a), with displacements <600 cm. (c) Histogram of fault dips, showing a range from <5 to 90°, with most in the range 35–80°, peaking at 60–65°. (d) Plot of fault dip against dip of planar bedding in adjacent footwall and hanging wall.

Fig. 2a) is within the Blue Lias. The Penarth Group (Tea Green Marl) is restricted to a small horst block in domain 7.

- Faults occur singly, in linked arrays, in splay systems or in extensional duplexes.
- In-plane displacement may be preserved across linked systems by bedding-parallel detachments (Fig. 6b), or lost via fracture splays, tip-line folds and damage zones (some which may reflect palaeo-tip line folds; McGrath and Davison, 1995).
- In the third dimension, faults may decay into en échelon normal faults linked by relay ramps (Walsh and Watterson, 1987; Peacock and Sanderson, 1991). Map-scale relay ramps are present (e.g. domain 9 where there is a homoclinal stratigraphy such as along strike from B14; Fig. 2a), but are less clear where there is significant reverse reactivation of normal faults or where bedding is folded on a scale greater than the overlap between two faults.

3.2. Structures formed by north–south contraction

The most common contractional structures are the partial reverse-reactivated steep normal faults and folds. Other contractional structures—neoformed thrusts (Figs. 7e and 10a) and localised grain-scale cleavage-formation (Fig. 7f)—are summarised in Table 3.

Table 3
Features of thrusts and cleavage

Neoformed thrusts unrelated to reactivated normal faults	Neoformed thrusts are scarce, occurring in both the Rhaetic (unit Rh) east of Lilstock (domain 12) and in Blue Lias (domains 2 and 3). Generally <1 m displacement (Fig. 10a). Larger (~100 m) thrust zones in the Blue Lias have well-developed calcite veins with slickenfibres and hanging wall anticlines and footwall synclines (Fig. 12e). Equal area plot of 16 neoformed thrusts gives a preferred orientation of 108°/16°N (Fig. 7e)
Cleavage	Rare in both the red Mercia Mudstone and Blue Liassic (localities in Fig. 2a). Morphology varies from grain scale, to axial surfaces to crenulations in bedding (Fig. 11f) represented in thin section by the short limbs of asymmetrical crenulations, to spaced cleavage. Equal area plot of seven cleavage readings give a preferred orientation of 109°/74°N (Fig. 7f)

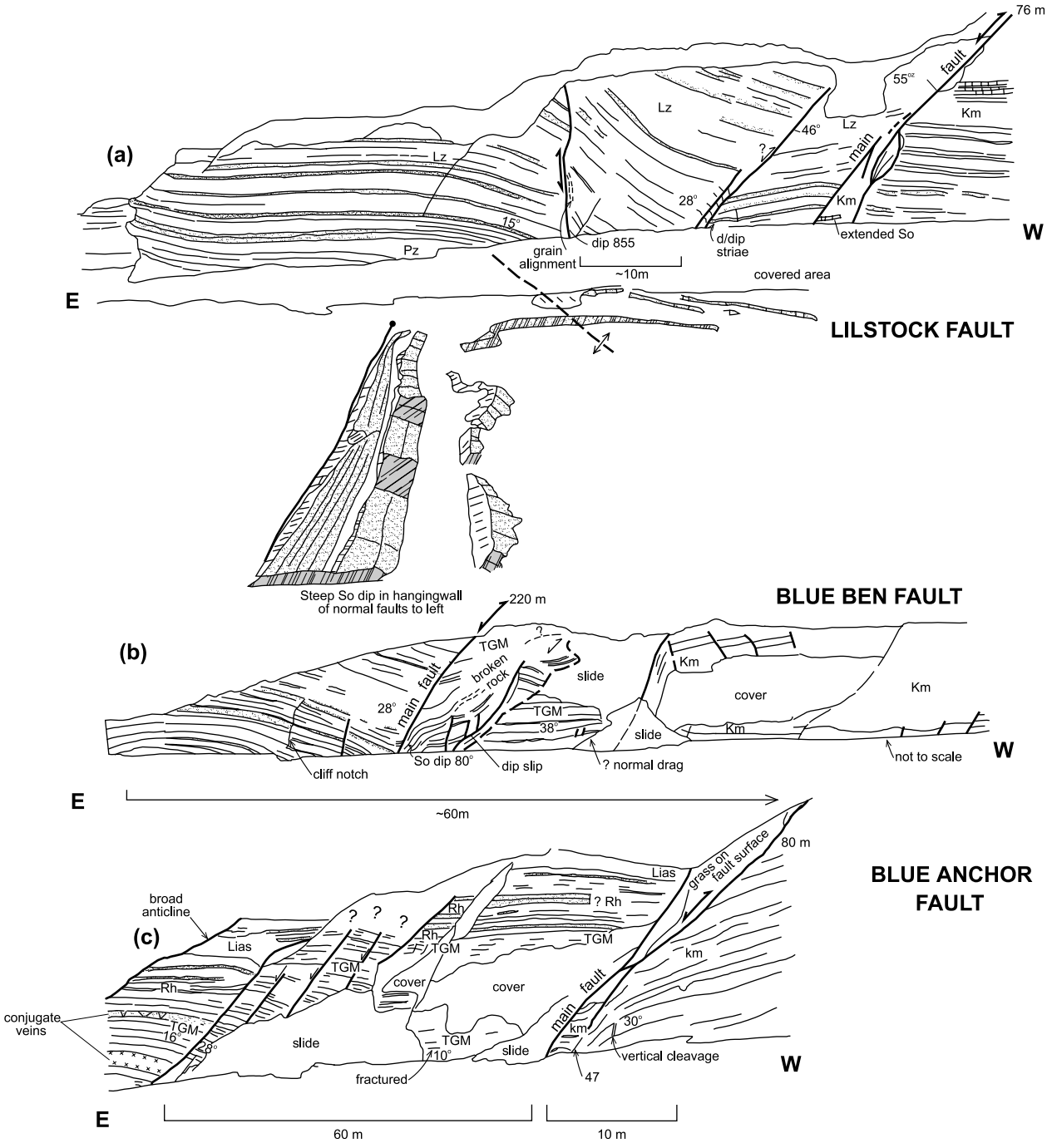

Fig. 9. Key features of the three of the largest faults in the basin margin. (a) The Lilstock Fault (maximum cliff line throw of ~76 m; Whittaker and Green, 1983). (b) The Blue Anchor Fault (~80 m throw; Edwards, 1999). (c) The Blue Ben Fault (maximum throw of ~220 m; Whittaker and Green, 1983). Curvature of bedding in footwalls is attributed to normal sense 'drag' folding. Hanging wall structures—low amplitude folds, local cleavage, reverse sense slickenfibres and in the Blue Anchor Fault, extensional conjugate gypsum veins (Hamilton and Whittaker, 1977; Davison, 1994)—are attributed to partial reverse reactivation.

3.2.1. Reverse reactivated planar normal faults. Key features of these faults are:

- Kinematic evidence of reverse reactivation, such as tool marks and slickenfibres with steps facing up-dip (Fig. 10b).
- The spread of orientation of contractional slickenfibres indicating that fault reactivation varies from pure reverse slip to oblique reverse slip (Fig. 7d). Oblique lineations on steep normal faults (Fig. 7g) might also be part of this deformation. The direction of reactivation can vary along individual planar normal faults (e.g. fault in domain Fig. 2a).
- Dip variation from 20 to 85°, generally 45 – 70° (Fig. 10c), indicating that reactivation was largely independent of fault dip.

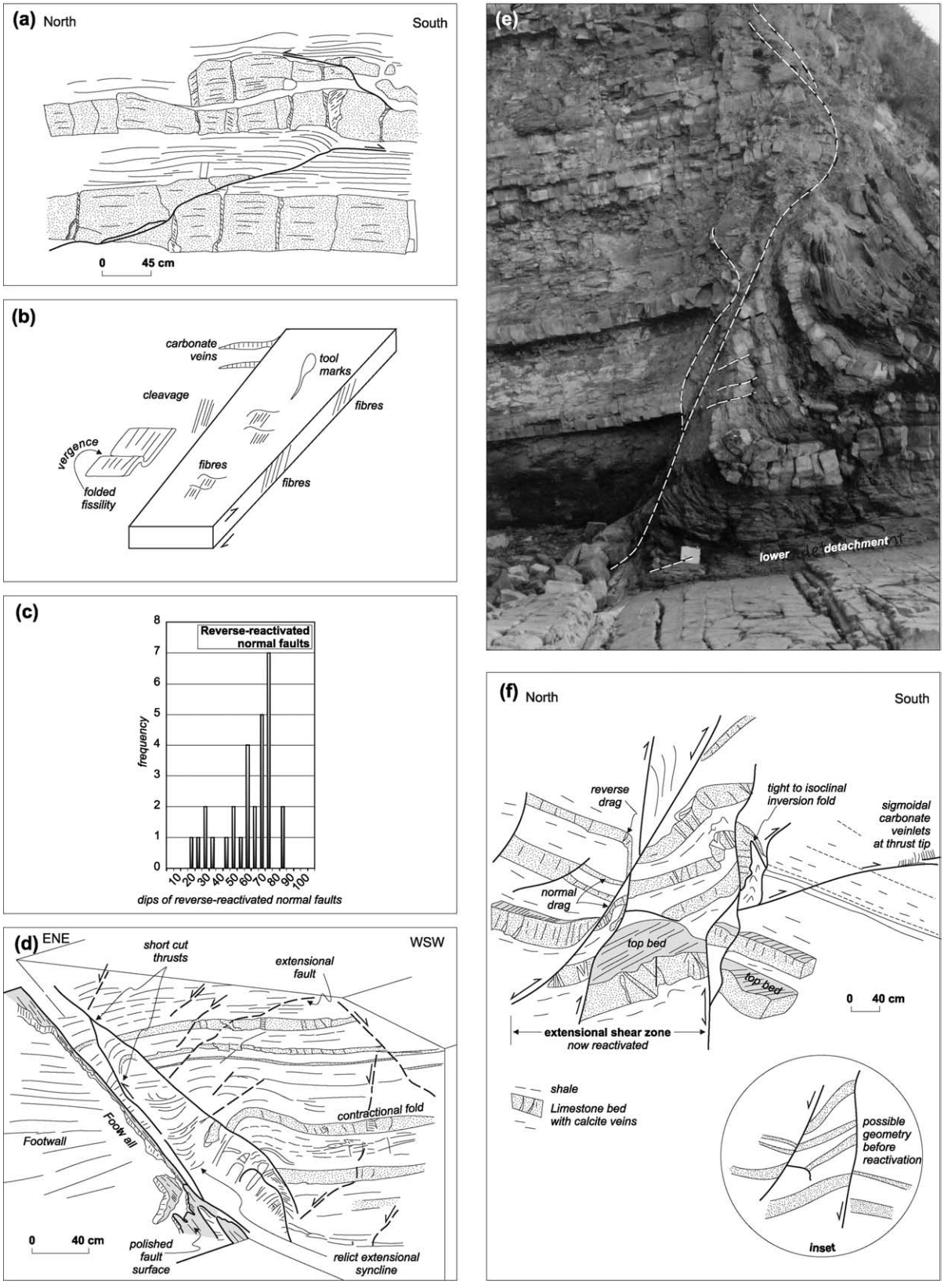

Fig. 10. Effects of contractional deformation. (a) Neoformed thrusts ramping through beds of limestone and shale and forming flats within shales. Note the hanging wall anticline developed in shale and limestone above the lower thrust. Unit Pz, Domain 3. (b) Schematic figure illustrating range of kinematic indicators used to indicate partial reactivation of planar normal fault. (c) Range of dips exhibited by partially reverse-reactivated planar normal faults with unequivocal reverse-sense kinematics. Comparison with Fig. 6c suggests that angle of dip exerted little control on which faults were reverse-reactivated.

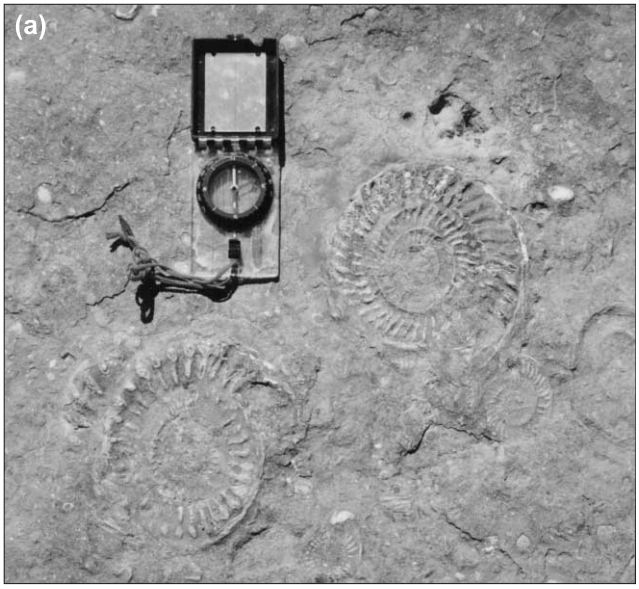

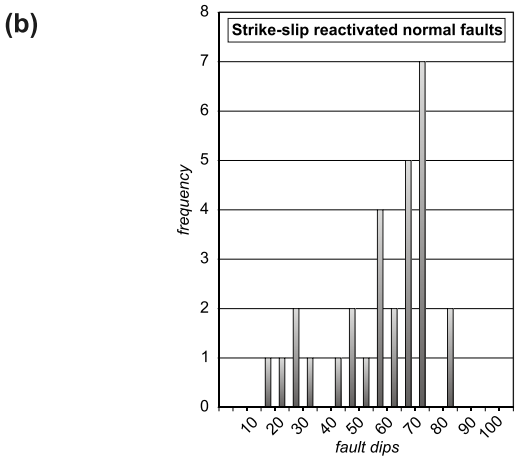

Fig. 11. (a) Variably deformed, elliptical ammonites elongate north–south. Unit Bz, domain 8, view looking north and down onto bedding surface. (b) Range of dips exhibited by partially strike-slip reactivated planar normal faults with unequivocal sub-horizontal kinematics.

- Maintenance of normal bedding separation of all but three faults. Only three reverse-reactivated faults show reverse separation of bedding, with the largest displacement being 8 – 9 m at the western end of the fault at Blue Ben (at A8, Fig. 2a).
- Presence of damage zones around some partially reactivated, steep planar normal faults. These may contain cleavage, folded shale fissility and splay extensional veins (Fig. 10b). Neoformed shortcut thrusts occur in the former hanging wall (Fig. 10d), footwall, and in former horse blocks. Contractional folds include asymmetrical synclines in footwalls of reactivated faults (Fig. 10e), anticlines in hanging walls (Fig. 10d) and tight folds in former extensional shear zones (Fig. 10f).

3.3. Structures formed by east–west contraction

Key features of these structures are:

- Subhorizontal slickenfibres and gently pitching striations (Fig. 7h) that in key areas (Fig. 2a; Appendix) overprint dip-slip extensional fibres in both the red Mercia Mudstone and the Blue Lias (Fig. 7g) (Hancock, 1985; Dart et al., 1995).
- Grain-scale east – west shortening reflected by the presence of deformed ammonites with long axes trending 006° (Figs. 7i and 11a).
- Variation in dips of partially reactivated planar normal faults, from <20 to 85°, generally 55 – 75° (Fig. 11b), suggesting that fault dip did not control which faults underwent strike-slip reactivation.
- Strike-slip reactivation of normal planar faults leading to flower structures (Davison, 1994).

3.4. Cross faults

Cross faults occur at all scales and are poorly grouped into a north to north-northwest-trending set and a northeast-trending set (Dart et al., 1995; Nemčok et al., 1995; Kelly et al., 1999) (Fig. 7j).

3.4.1. North to north-northwest-trending set. Key features of this set are:

- Faults with dextral strike-slip separation of bedding and dextral strike-slip kinematics (Dart et al., 1995; Kelly et al., 1999).
- Normal faults with down-dip and oblique-slip lineations (Fig. 7k).
- Faults with both oblique dextral reverse and strike-slip movement.
- Faults with reverse dip-slip striations.

Good examples of these faults at map scale occur on both sides of, and include, the dextral Watchet Fault west of Watchet (Fig. 2a). Other examples occur in the rotated

(d) Partially reactivated planar normal fault showing slickenfibres on fault surface (shaded). Hanging wall contains an inversion anticline cut by synchronous or younger extensional faults. Anticline is also cut into two short-cut thrusts that bound a horse with a relict hanging wall syncline. Short cut faults join the reactivated main fault above the field of view. Unit Bz, Domain 8 east of Kilve Pill. (e) Reactivated steep normal fault at Blue Ben. Footwall contains inversion syncline with thrusts in the hinge and shallow dipping normal faults in the thinned steeply dipping limb. Lower detachment is present below the syncline. An early extensional history on this fault is suggested by the hanging wall anticline preserved on the rock platform (Nemčok et al., 1995). Units Az and Bz, Domain 3, view looking west, clipboard for scale. (f) Strongly reverse-reactivated extensional shear zone. Beds within shear zone show inversion folds, and inversion anticline overprints extensional syncline in former hanging wall. Inset shows inferred geometry shear zone before reactivation. Neoformed segmented thrust in footwall on RHS contains sigmoidal calcite veinlets at the tip (see McGrath and Davison, 1995). Unit Bz, domain 8.

anticlinal limb in the western part of domain 3, and cutting across folded limbs of Muddy Syncline in domain 13 (Fig. 2a).

3.4.2. Northeast-trending set. Key features of elements of this set are:

- General sinistral displacement, generally between 0.5 and 2 m (Kelly et al., 1999; Fig. 3a), but up to 25 m (Az/Bz boundary in domain 5 (Fig. 2a).
- Presence of some faults with strike-slip (dextral) kinematics (Fig. 7k) and evidence of multiple movements.
- Apparent normal separation of bedding in cliff section because of the very gentle bedding dips.
- Occurrence of faults in zones that cut across WNW folds and faults (Fig. 2a). East of Watchet (domain 2), these faults are associated with NE folds that reflect strain accommodation in the footwall of Helwell Bay East Fault. In the eastern part of domain 4 and in domain 5, a swarm of NE-trending faults cut a regional fold hinges and rotated limbs.
- Cross faults are more prevalent in stratigraphic units such as unit Az that are limestone rich (domain 5).
- NE-trending faults terminate on, as well as truncate, E–W faults (also Kelly et al., 1999).

3.5. Overprinting relationships

Several different types of overprinting relationships have been recognised:

- Multiple formation of extensional faults, generally restricted to 'steep' bedding (dips of 13–20°, compared with normal dips of less than 10°). Early, shallowly dipping planar and listric normal faults are cut by younger steeply dipping normal faults (e.g. domain 10, steep limb Range Station Anticline, and domain 9) (Fig. 2a and b). Steep planar extensional faults may nucleate on shallow ones. The early faults include subhorizontal faults with ramp-flat geometries, and low to moderate cut-off angles with bedding (Fig. 12a and b).
- Partial reverse reactivation of planar normal faults (Fig. 10d).
- Partial strike-slip reactivation of planar normal faults.
- Neoformed thrusts overprinting normal faults, with the earlier faults either folded (Fig. 12c) or truncated by the thrusts (Fig. 12d).
- Late extensional faults cutting neoformed thrusts (Fig. 12e).
- Rotation of earlier formed cleavage in synclines that lie in the hanging walls of late normal faults (Fig. 12f).

3.6. Folds and fold-fault relationships

In both plan and section, regional folds are commonly non-cylindrical over along strike distances <300 m: they show abrupt changes in amplitude, wavelength and plunge along strike. The resulting variation in geometry is accompanied by abrupt changes in displacements along the sub-parallel faults, most clearly seen in the overlapping profile sections of Fig. 5. The partially reactivated steep normal faults parallel to fold axial traces may breach the actual hinge (e.g. domain 14 in Fig. 2a).

We recognise three different regional fold-fault associations.

3.6.1. Normal-sense fold pairs decorating planar normal faults.

- These consist of hanging wall synclines and footwall anticlines.
- These folds provide a component of ductile extension superimposed on fault displacement (cf. Walsh and Watterson, 1990; Peacock and Sanderson, 1991).
- Wavelengths range from 10–50 cm around small faults to $\sim$30 m, and amplitudes of <6 m on the margins of faults with larger displacements.
- Rotated bedding close to the fault may be thinned by solution transfer.
- Changes in the plunges reflect a displacement gradient along the fault from the centre to the tips (cf. Barnett et al., 1987; Walsh and Watterson, 1990; Peacock and Sanderson, 1994) (Fig. 13a). Good examples occur in domain 2 along the Helwell Bay Fault (A. Beach, personal communication, 2000) and in domains 8 and 9, along the Quarry Fault (domain 12) and the No-Name Fault (domain 13).

3.6.2. Anticlines. Anticlines with amplitudes of generally <20 m in the hanging walls of partly reactivated normal faults are contractional because:

- They have the opposite vergence to mesoscopic extensional fold pairs that are characterised by synclines in fault hanging walls.
- They are accompanied by the presence of local cleavage, limb dips from 5 to 85° and interlimb angles from $\sim$110 to 160°.
- Fold hinges are elevated above their regional (see below). Examples include those in the hanging wall of the Quantocks Head Fault (boundary between domains 4 and 5, Fig. 2a) (Davison, 1994; A. Beach, personal communication, 1994; Kelly et al., 1999) and open syncline–anticline pairs in the hanging walls of the major faults in Fig. 9.
- Many of these contractional folds contain fanning extensional faults in their hinge areas, especially in the more competent strata of units Pz and Az. These faults die out above or below in the muddy unit Lz (e.g. domain 12, Fig. 2a) (Fig. 13c and d).

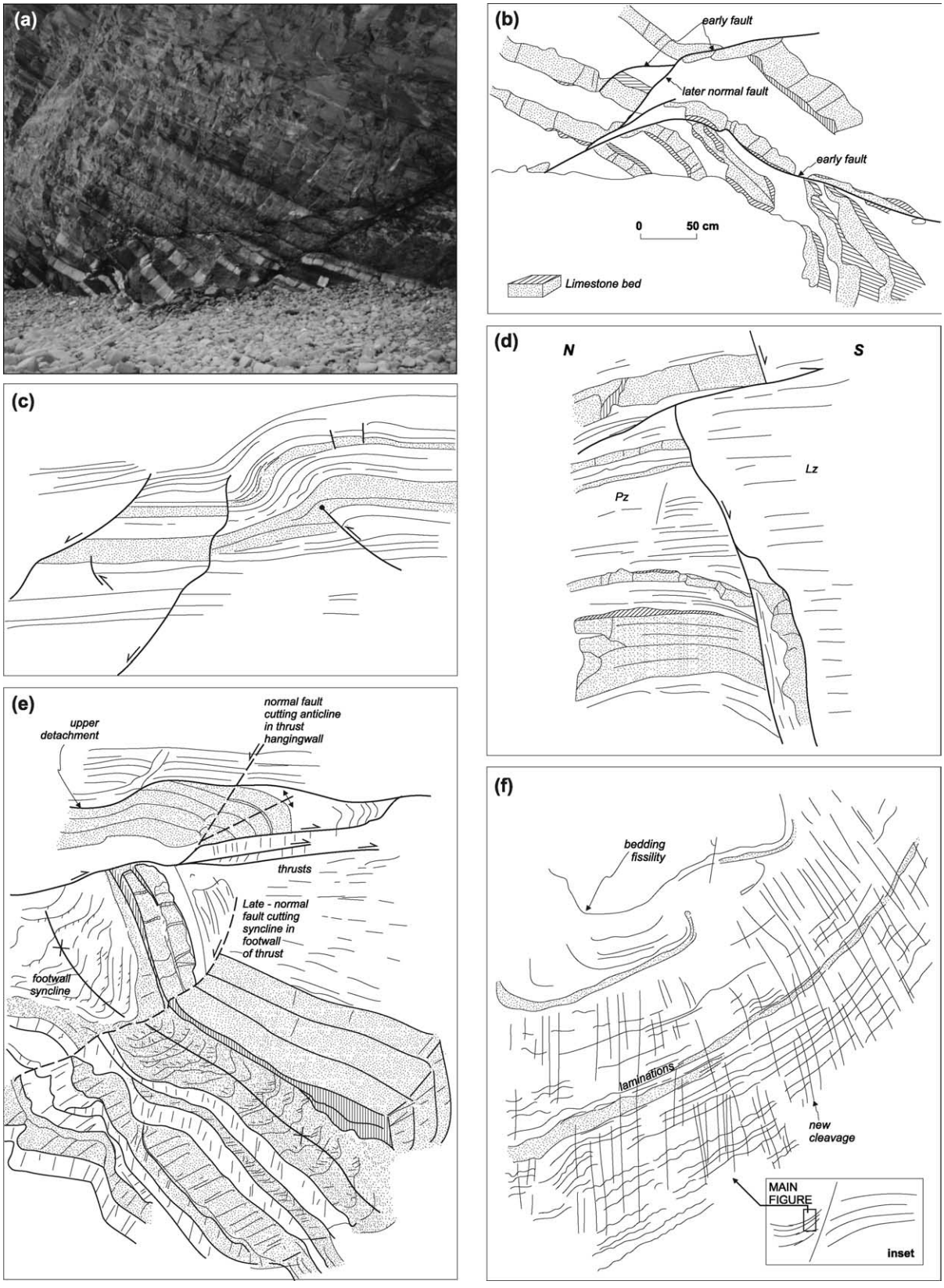

Fig. 12. Mesoscopic overprinting relationships. (a) Early shallow planar normal fault, cut by steep planar fault on RHS and containing steep normal fault in footwall on LHS. Unit Bz, domain 10. View looking east, clipboard for scale. (b) Detail of part of footwall from LH bottom above, showing early normal fault, with hanging wall flat and footwall ramp, rotating on LHS into steeper normal fault (with hanging wall and footwall ramps) and cut by later normal fault. Unit Bz, domain 10. (c) Opposite verging normal faults and thrust cored fold pair. Irregularly shaped normal fault in centre of figure is interpreted to predate

Range Station Anticline. The classic Range Station Anticline (domain 10, Fig. 2a and b) is interpreted as an inversion fold, although preserving relics of an earlier geometry as a hanging wall fold formed during extension on the Range Station Fault. The geometry of this fold and the Range Station Fault changes markedly along strike. Dips of the fault shallow from 84–75° near its western end to 55° near the cliff line. Concurrent with this is the elevation of the anticline in the west, as shown in the profile sections B18–B19, B20–B21, B22–B23 (Fig. 5), which is consistent with formation as an inversion fold. However, the cliff line section (Fig. 2b, A19–A23) shows the southern limb of the fold is depressed below the regional, consistent with formation either as a rollover fold above a listric normal fault (as originally interpreted by Hancock (1985)) or as, preferred here, a hanging wall fold above a planar normal fault (cf. Fig. 13a). Tightening of the fold during partial contractional reactivation of the Range Station Fault post-dates formation of early normal faults in the southern limb that were subsequently rotated into subvertical and subhorizontal dips.

3.6.3. Regional fold trains. Fold trains dominate the eastern part of the basin margin, east of Lilstock, (Fig. 2a) and domains 9–5 to the west, where regional fold pairs are parasitic with respect to a regional synclinorium centred on the Kilve Syncline in domain 8 (Fig. 13b and c). The amplitude of this fold, ~72 m measured in unit Az, is greater than the displacements of smaller scale normal faults that mostly downthrow to the north, antithetic to the limb dip (Fig. 2b). South- and north-dipping fold limbs occur between Kilve Pill and St Audries Bay in the west of the basin margin.

The large broad anticline in Saint Audries Bay west of Blue Ben Fault, St Audries Bay (domain 3), is another example where the fold amplitude of ~225 m is much greater than the <5 m displacements of steep normal faults cutting it (Fig. 2a, Fig. 5, B4–B7).

Beds farther west lie in the strongly rotated limb straddling the domain 2/3 boundary. Most of domain 2 is characterised by northerly dips in the Blue Lias in the hanging wall of the Helwell Bay Fault, whereas domain 1, west of the Watchet Fault, contains partially fault-disrupted regional folds.

4. Discussion: inversion of the southern margin of the Bristol Channel

By working on the exhumed southern margin of the Bristol Channel Basin, we have been able to identify processes that were active during the early stages of basin inversion. Here, we synthesise the structural history of the southern margin of the Bristol Channel Basin, firstly in terms of a deformation sequence, and then in relation to the three models discussed in the introduction of the paper.

Our preferred deformation history for the southern margin of the Bristol Channel Basin (Fig. 14) is based on the constraints provided by extensional, contractional and strike-slip structures above, and their overprinting relationships summarised above and detailed in the data supplement. Key constraints are the normal separation of >95% steep normal faults despite their reverse reactivation, the presence of regional contractional folds and presence of multiple generations of extensional faults. Because the deformation history below is dependent upon estimating how many and which extensional faults formed at which time, it is possible to erect variants in which more or fewer extensional faults occurred in each phase of deformation.

We begin with the first set of extensional faults (Fig. 14a). With some uncertainty, we identify these as the large displacement faults that throw Blue Lias down against the Mercia Mudstone Group. These faults are planar and they lack obvious growth, as recorded by similar thicknesses of Blue Lias in footwalls and hanging walls (but note the restricted section perpendicular to strike). Three features suggest that these extensional faults did not occur during deposition of Triassic and Early Jurassic strata: the absence of soft sediment structures in the Blue Lias; the presence of crack-seal fracturing and veining of limestone beds (Dart et al., 1995; Davison, 1995); and the deposition of the Blue Lias during regional sag phase subsidence after a Triassic rifting event (Tappin et al., 1994). These early extensional faults probably formed in the Late Jurassic, when the Blue Lias was covered by ~1700 m of overlying strata (Tappin et al., 1994). Rare listric and ramp-flat faults may have also formed during this event.

The limited lineation data on the major faults (Figs. 2a and 7) suggest the direction of Late Jurassic maximum extension was oriented NNE–SSW (also Dart et al., 1995). An unknown number of planar smaller normal faults and lineations may have also formed in this first phase of extension.

Extension was followed by inversion of the basin margin, the first sign of which was the kinematic evidence for reverse-reactivation of the extensional faults described above, which are still in net extension (Fig. 14b). Before these faults could pass into contraction at the level of observation, the dominant process of inversion switched from shortening accommodated by contractional slip on

thrusting, and to have been partly displaced by northward vergent fold pair cored by a south-dipping thrust. Units Rh and Pz, domain 12. (d) Decapitation of steep normal fault by low angle basinward dipping neoformed thrust unit Lz on right and Pz on left, domain 12. (e) Neoformed N-dipping complex thrusts containing calcite veins with reverse sense fibres. Hanging wall anticline is cut by post contractional basinward-(N) dipping normal fault. Footwall of thrust contains syncline that is cut by listric extensional fault. Unit Rh, domain 12. (f) Rotated cleavage and bedding laminations in syncline in hanging wall of planar normal fault. Unit Pz, domain 12. Inset gives broader view of syncline in hanging wall of normal fault.


(a)

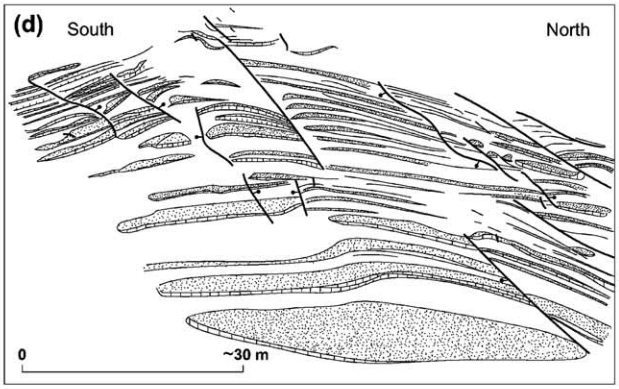
(d)
South
North
0
~30 m

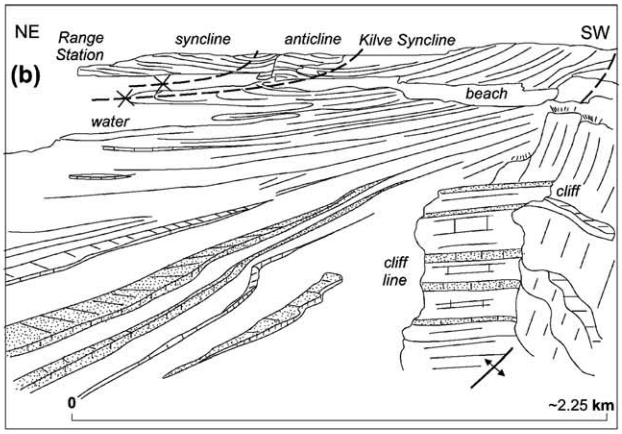
NE
Range Station
syncline
anticline
Kilve Syncline
SW
(b)
beach
water
cliff
cliff line
0
~2.25 km


(c)
60°
40°
70°
70°
80°
65°
53°
74°
80°
85°
55°
47°

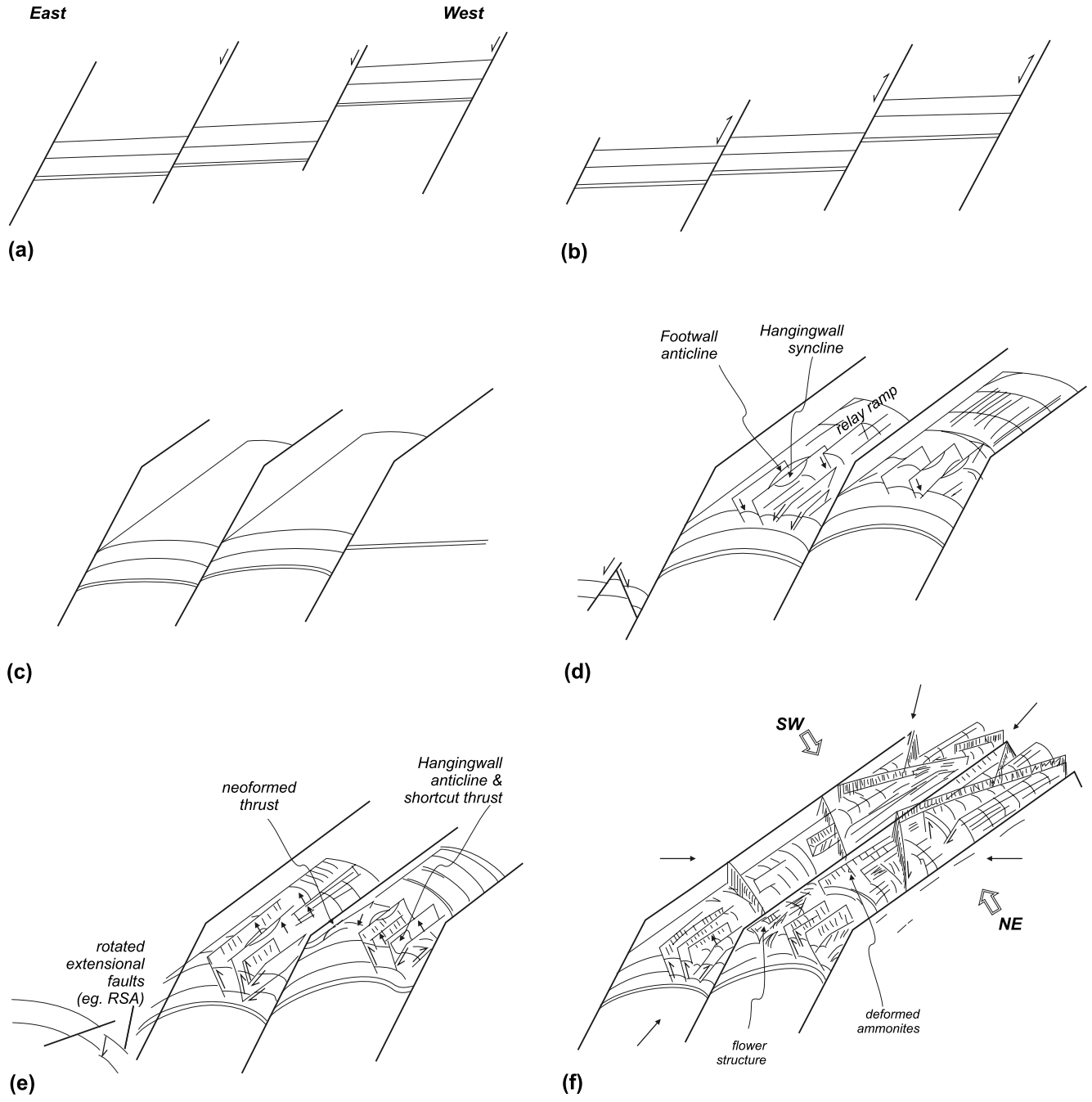

Fig. 14. Summary figure illustrating sequence of structuring of the southern margin of the Bristol Channel Basin. See text for descriptions.

discrete old faults to distributed bulk shortening ('pure shear'), reflected by the ductile folding of those blocks between these reactivating faults (Fig. 14c). In this second stage of inversion, folding was accompanied by outer arc extension that led to the generation of planar normal faults, some of which were flanked by normal sense folds (Fig. 14d). With progressive tightening of folds, finite neutral surfaces migrated into fold cores (Ramsay and

Fig. 13. Folds. (a) Doubly plunging map-scale syncline and anticlines in footwall and hanging walls, respectively, of steep planar normal faults. Plunge variations reflect displacement gradients along fault from centre towards tips. Unit Az in foreground, Bz in background, domain 8, view looking west, width of photo ~50 m. (b) regional folds, looking east towards Kilve and the Range Station showing the presence of two regional synclines, intervening anticline and second anticline on right of figure. Width of figure ~2.25 km. (c) detail of LHS of (b), showing syncline–anticline pair and fanning planar normal faults. Field of view ~1.3 km. (d). Sketch of anticlinal hinge, with planar normal faults showing predominant fanning in dips across hinge. Rhaetic, domain 12.

Huber, 1987, p. 461), and normal faults grew downwards within fold hinges, resulting in multiple growth stages, as recognised by McGrath and Davison (1995). Where folds tightened to produce limb dips of 20–30°, outer arc normal faults were passively rotated into subhorizontal or subvertical dips, unsuitable for further slip, and became inactive (left hand side Fig. 14d and e). New outer arc normal faults formed cutting the older faults (e.g. in the steep southern limb of the Range Station Anticline, A22, Fig. 2a). Structural data, therefore, lead to a picture of blocks bounded by the large planar normal faults moving initially 'back up' those faults, then becoming internally shortened by folding, and then undergoing fragmentation largely on strike-parallel, outer-arc normal faults. Bedding-parallel shear veins may have formed at this time, reflecting slip during folding.

Our model of fault-formation implies that many planar normal faults formed during contractional folding. Support comes from the fanning of normal faults around anticlinal hinges (Fig. 13c and d). This roughly perpendicular relation between these faults and bedding is difficult to achieve if the normal faults formed in horizontal bedding at Andersonian dips ($\sim$60°). It is more explicable if the faults formed during folding or after initial fold formation. Map-scale data showing close relationships between faults and folds, with both undergoing similar abrupt variations in geometry along strike, also support formation of faults at this time.

Kinematic evidence for the reverse-reactivation of outer-arc steep normal faults marks a third stage in basin inversion, with shortening concentrated on discrete small–medium displacement faults distributed along the margin (Fig. 14e). Data in Fig. 10c indicates that faults with normal displacements as little as 2 m were partially reactivated. Orientation data indicate that contractional lineations on partially reverse-reactivated normal faults reflect a NNE–SSW direction of maximum shortening (Fig. 7d), consistent with previous work (Dart et al., 1995; Nemčok et al., 1995; Kelly et al., 1999). Lineation data, however, also indicate an oblique component to the deformation (Fig. 7d and g, and this is reinforced by subhorizontal, strike-slip striae (Fig. 7h) on some steep normal faults.

Is there a relationship between the strike of a steep normal fault and its mode of reactivation? Kelly et al. (1999) envisaged local transpression on curved faults around the Quantocks Head Fault, with more strike-slip on ends and more contraction in the centre. We suggest that their conclusions on the interaction of partly reactivated normal faults and strike-slip faults at Quantocks Head are consistent with a regional scale pattern of complex three-dimensional deformation reflecting: (i) a NE (oblique) direction of maximum shortening that was partitioned into reverse, oblique and strike-slip reactivation on steep planar normal faults. This oblique direction of maximum shortening accounts for the east–west, grain-scale shortening of ammonites (Fig. 7i), the local presence of reverse and strike-slip striae on the same fault surface (both overprinting steep normal sense striae); (ii) strain variations set up by strike and dip variations of the E–W faults and the significant non-cylindrical nature of flanking folds that vary in plunge, amplitude and wavelength along strike; (iii) generation of cross faults that play a significant part in basin deformation by acting as hard boundaries that help to partition and accommodate this three-dimensional non-coaxial deformation. We thus agree with Nemčok et al. (1995) and Kelly et al. (1999) that strike-slip faulting was synchronous with (the latter stages of) contractional reactivation (Fig. 14f), rather than the view of Dart et al. (1995), which suggested that these NE faults post-dated E–W faulting.

Both Dart et al. (1995) and Kelly et al. (1999) suggested that the NE and the N-NNW cross faults are conjugate (sinistral and dextral, respectively) and formed in response to N–S shortening. However, the presence of down-dip and oblique-slip normal striations (Fig. 7k) indicates more complex fault movements, at least locally. They probably reflect localised near-field NW–SE and ENE–WSW components of extension during the later stages of basin contractional deformation (Fig. 14f).

One implication of our three-stage model is that whereas the mesoscopic hanging wall syncline and footwall anticline folds that commonly flank planar normal folds formed during extension, most map-scale folds formed during inversion, with reverse sense of asymmetry and the elevation of anticlinal hinges above the 'regional'. In some cases, they formed from pre-existing extensional folds. Different scale folds thus formed at different times.

Late stage, minor extension produced post-contractional normal faults. Examples include normal faults cutting neoformed thrusts and the rotation of folded and cleaved shales (related to a neoformed thrust) in an extensional shear zone.

5. Comparison with models of basin inversion

In this section, we use key data from the Bristol Channel Basin to test the applicability of inversion models summarised in Section 1.

5.1. Reactivation of growth fault model

This process seems to apply to the southern margin of the Bristol Channel Basin, where steep normal faults, although not forming during Early Jurassic growth, show kinematic evidence for reverse reactivation. The simplest explanation why 95% of these faults still show normal stratigraphic separation is that the faults at our level of the observation lie below their null points.

This explanation, however, can only apply to those large faults that extended up into younger, now eroded, strata. It is

logical to assume that at higher stratigraphic levels above their null points, these faults would lie in net contraction. With further shortening, null points would move down the faults into Lower Jurassic and Triassic strata, and the large normal faults would become reverse faults as the basin margin was inverted.

This process does not apply, however, to those partially reverse-reactivated, steep normal faults wholly contained in cliff sections and which lie in net extension from top to bottom. Reverse-reactivation of these faults must have ceased at an early stage. This is consistent with the widespread presence of flanking shortcut structures that suggest that these faults had become locked up due to waning stresses, increasing friction due to steepening of fault dips, reduction of fluid pressure (Sibson, 1995), or strain-hardening due to calcite veining (Davison, 1994).

5.2. Thin-skinned model

The presence of neoformed thrusts indicates that this process has occurred along the southern margin of the Bristol Channel Basin, but it was largely restricted to the mesoscopic scale: with one exception, there are no regionally mappable thrusts.

5.3. Buttress model

Application of the buttress model to the Bristol Channel Basin—to the Quantocks Head Fault by Beach (personal communication, 1994), to the southern margin in general by Dart et al. (1995) and Nemčok et al. (1995)—implies that anticlinal folds and abnormal shortenings only occur in the hanging walls of those old faults, and that there was a mechanical contrast, at least temporarily, across these faults during inversion.

While there are hanging wall anticlines like the Range Station Anticline (domain 10) (see below), data from Figs. 2a and b and 5 show that regional anticlines are not restricted to fault hanging walls. Regional footwall anticlines occur in domain 14 (at Benhole Point) in the footwall of the No-Name Fault, which also has a hanging wall anticline (domain 13), in domain 5 (eastern side) in the footwall of the Quarry Fault (domain 12), in the footwall of the Lilstock fault (domain 11), and in domain 4, where the anticline in the footwall of the Quantocks Head Fault has a greater amplitude than the anticline in the hanging wall (Figs. 2a and b and 5).

Nor does there appear to have been major permanent mechanical contrast across faults that have hanging wall anticlines. In the Range Station Anticline, both the hinge of the anticline and the footwall of the Range Station Fault occur in the same lithostratigraphic unit (unit Az). Limited amount of unit Bz only occurs in the immediate hanging wall, but also occurs at the cliff tops in the footwall. In the Quantocks Head Fault example, the hanging wall (unit Bz, shale/limestone ratio ~8.7:1) is more competent than the footwall exposed in the core of the large anticline on the rock platform (unit Lz with a shale/limestone ratio of ~14:1) although the local footwall is more competent (unit Az, shale/limestone ~2.6:1).

5.4. Distributed deformation model

The constraints imposed by outcrop and map scale data point to a new model, the distributed deformation model, in which shortening of the Blue Lias between the early, partially reactivated faults was accomplished by folding distributed over most of the basin margin. The dominance of folding is best expressed by the regional synclinorium that extends from domain 5 to domain 9. This fold, with an amplitude of 72 m (>maximum fault displacement in the limbs) contains several second order folds (Figs. 2a, 5 and 13b and c) that contain fanning extensional faults. Folding was accompanied by outer-arc normal faulting, and the formation of small neoformed thrusts. Grain-scale strain is revealed by deformation of ammonites. Subsequent deformation was accomplished by minor reverse reactivation of the distributed outer arc faults.

In the distributed deformation model, shortening of basin-fill is accomplished by strain distributed relatively evenly across the high levels of the deforming basin. Support comes from Sibson (1995) who suggested that the lock-up of older faults could lead to distributed strain at high levels that may contribute to the development of antiformal buckle folding. Thus sealing of early faults may cause a change in deformation mechanisms. This model finds support from the clay models of Eisenstadt and Withjack (1995) which, at 44–50% inversion of a half graben, showed at a high level the formation of a low amplitude anticline flanked by neoformed thrusts. Deeper down, inversion was accomplished by very limited reverse reactivation of selected growth faults. Between 50 and 100% of inversion, the contractional reactivation of the main normal fault ceased to be the main process of basin inversion and was replaced by a generation of distributed low angle thrust faults with small displacements. Distributed deformation has been described from basins that contain significant salt layers. Harvey and Stewart (1998) and Smith and Hatton (1998) reported that the presence of a salt layer favoured the 'delocalization' of inversion deformation leading to the formation of folds, general uplift and conjugate faults over a wide area.

6. Conclusions and implications

The southern margin of the Bristol Channel Basin is dominated lithologically by mechanically weak mudstones interbedded with limestone beds. In the Early Jurassic Blue Lias Formation, it is dominated structurally by regional WNW-trending, non-cylindrical folds and normal faults, the latter forming in response to Late Jurassic N–S extension.

Processes involved in the inversion of the southern margin of the Bristol Channel Basin are severely constrained by the fact that these steep faults still lie in stratigraphic extension, even though they show widespread kinematic evidence of some reverse reactivation. We suggest basin inversion occurred in three stages, but it is unclear how these stages relate to the three exhumation events of Holford et al. (2005). The first stage of basin deformation commenced by the reverse reactivation of major (>70 m) normal faults. These faults lie in net extension because at the level of observation (Lower Jurassic and Triassic) they lie below their null points. Before stratal contraction could migrate further down these faults, reverse reactivation on them ceased. In the second stage of inversion, blocks between the major faults underwent shortening by major folding and local grain scale deformation. There is little evidence that contractional folds only formed as buttress folds: regional inversion folds are associated with both hanging walls and footwalls of old planar normal faults and probably formed as trains of folds during distributed shortening. Most of the mesoscopic steep planar normal faults occurring in the hinges of regional folds probably formed during this part of the deformation, during outer arc extension in the developing folds. This stage of deformation was by bulk pure shear shortening.

Deformation in the third stage was brittle and concentrated on the mesoscopic steep normal faults. A NE–SW direction of maximum shortening was partitioned into reverse, oblique and strike-slip reactivation of older normal faults. The contractional folds and the partially reactivated normal faults underwent segmentation caused by a combination of non-planar faults, cross faults and fanning outer arc extensional faults.

The difference between this three-stage distributed deformation model of basin-inversion model and other inversion models might reflect the muddy fill of the Bristol Channel Basin that was capable of undergoing significant ‘pure shear’ by folding as well as limited fault reactivation.

Acknowledgements

This project was funded by the Australian Department of Industry, Technology and Development, the Geological Survey of New South Wales and the Geology Department University of Bristol. We thank several people for discussion in the field or office: Jacques Angelier, Ian Davison, Alastair Beach, Richard Lisle, John Walsh, and David Tappin and Richard Edwards also for pre-publication copies of their work. The manuscript benefited from the helpful constructive comments and reviews by Chris Mawer, Paul Lennox, Alastair Beach, Jonathan Turner (several times!) and Tom Blenkinsop. The seismic section is courtesy of Geco-Prakla (UK). The colour map was produced by Cheryl Hormann, Li Li, Barbara Bulanowski and Trisha Moriarty (Geological Survey of New South Wales) Published with the permission of the Deputy Director-General Minerals New South Wales, Department of Primary Industries and the Director of the British Geological Survey.

Although Paul Hancock was not able to see this final version of our paper, he did co-author joint abstracts and early drafts, and he and Glen field-tested the map together in September 1997. This paper reflects his interest, dating back to the early 1980s, in extensional tectonics in this classic area.

References

Angelier, J., 1994. Fault slip analysis and palaeostress reconstruction. In: Hancock, P.L. (Ed.), Continental Deformation. Pergamon Press, Oxford, pp. 53–100.

Badley, M.E., Price, J.D., Backshall, L.C., 1989. Inversion reactivated faults and related structures: seismic examples from the southern North Sea. In: Cooper, M.A., Williams, G.D. (Eds.), Inversion Tectonics. Geological Society, London, Special Publication 44, pp. 201–219.

Barnett, J.A.M., Mortimer, J., Rippon, J.H., Walsh, J.J., Watterson, J., 1987. Displacement geometry in the volume containing a single normal fault. Bulletin of the American Association of Petroleum Geologists 71, 925–937.

Bishop, D.J., Buchanan, P.G., 1995. Development of structurally inverted basins: a case study from the West Coast, South Island, New Zealand. In: Buchanan, J.G., Buchanan, P.G. (Eds.), Inversion Tectonics. Geological Society, Special Publication 88, pp. 549–585.

Brodie, J., White, N., 1994. Sedimentary basin inversion caused by igneous underplating: northwest European continental shelf. Geology 22, 147–150.

Brooks, M., Trayner, P.M., Trimble, T.J., 1988. Mesozoic reactivation of Variscan thrusting in the Bristol Channel area, U.K.. Journal of the Geological Society, London 145, 439–444.

Buchanan, J.G., Buchanan, P.G. (Eds.), 1995. Basin Inversion Geological Society London Special Publication 88. 596pp.

Butler, R.W.H., 1989. The influence of pre-existing basin structure on thrust system evolution of the Western Alps. In: Cooper, M.A., Williams, G.D. (Eds.), Inversion Tectonics. Geological Society, London, Special Publication 44, pp. 105–122.

Cartwright, J.A., 1989. The kinematics of inversion in the Danish Central Graben. In: Cooper, M.A., Williams, G.D. (Eds.), Inversion Tectonics. Geological Society, London, Special Publication 44, pp. 153–175.

Cooper, M.A., Williams, G.D. (Eds.), 1989. Inversion Tectonics. Geological Society, London, Special Publication 44. 375pp.

Cornford, C., 1986. The Bristol Channel Graben: organic geochemical limits on subsidence and speculation on the origin of inversion. Proceedings of the Ussher Society 6, 360–367.

Cosgrove, J.W., 2001. Hydraulic fracturing during the formation and deformation of a basin: a factor in the dewatering of low-permeability sediments. Bulletin of the American Association of Petroleum Geologists 85, 737–748.

Coward, M.P., 1994. Inversion tectonics. In: Hancock, P.L. (Ed.), Continental Deformation. Pergamon Press, New York, pp. 280–304.

Dart, C.J., McClay, K.R., Hollings, P.N., 1995. 3D analysis of inverted extensional fault systems, southern Bristol Channel Basin, UK. In: Buchanan, J.G., Buchanan, P.G. (Eds.), Basin Inversion. Geological Society, London, Special Publication 88, pp. 393–413.

Davison, I., 1994. Structural geology field guide to the Watchet–Lilstock area, Somerset and Hartland Quay, N. Devon, Department of Geology, Royal Holloway, University of London, Egham, Surrey. Unpublished.

Davison, I., 1995. Fault-slip evolution determined from crack-seal veins in pull-aparts and their implications for general slip models. Journal of Structural Geology 17, 1025–1034.

Edwards, R.A., 1999. The Minehead district—a concise account of the geology. Memoir for 1:50,000 Geological Sheet 278 and part of sheet 294 (England and Wales). British Geological Survey. The Stationery Office, London.

Eisenstadt, G., Withjack, M.O., 1995. Estimating inversion: results from clay models. In: Buchanan, J.G., Buchanan, P.G. (Eds.), Basin Inversion. Geological Society, Special Publication 88, pp. 119–136.

Engelder, T., Peacock, D.C.P., 2001. Joint development normal to regional compression during flexural flow folding: the Lilstock buttress anticline, Somerset, England. Journal of Structural Geology 23, 259–277.

Gillcrist, R., Coward, M., Mugnier, J.L., 1987. Structural inversion and its controls: examples from the Alpine foreland and the French Alps. Geodinamica Acta 1, 5–34.

de Graciansky, P.C., Dardeau, G., Lemoine, M., Tricart, P., 1989. The inverted margin of the French Alps and foreland basin inversion. In: Cooper, M.A., Williams, G.D. (Eds.), Inversion Tectonics. Geological Society Special Publication 44, pp. 87–104.

Hamilton, D., Whittaker, A., 1977. Coastal exposures near Blue Anchor, Watchet and St Audrie's Bay, North Somerset, Field Guide 1977 pp. 101–109.

Hancock, P.L., 1985. Locality 2. Watchet coast section. In: Hancock, P.L. (Ed.), Extensional Tectonics in Southern England. Preconference Excursion (12–14 April 1985) of the Conference on Continental Extensional Tectonics, University of Durham, April 18–20 1985. Geological Society, London (unpublished), p. 4.

Harvey, M.J., Stewart, S.A., 1998. Influence of salt on the structural evolution of the Channel Basin. In: Underhill, J.R. (Ed.), Development, Evolution and Petroleum Geology of the Wessex Basin. Geological Society, London, Special Publication 133, pp. 241–266.

Hillis, R.R., 1992. A two layer lithospheric compressional model for Tertiary uplift of the southern United Kingdom. Geophysical Research Letters 19, 573–576.

van Hoorn, B., 1987. The South Celtic Sea/Bristol Channel Basin: origin, deformation and inversion history. Tectonophysics 137, 309–334.

Holford, S.P., Turner, J.P., Green, P.F., 2005. Reconstructing the Mesozoic–Cenozoic exhumation history of the Irish Sea basin system using apatite fission track analysis and vitrinite reflectance data. In: Dore, A.G., Vining, B.A. (Eds.), Petroleum Geology: North-West Europe and Global Perspectives—Proceedings of the Sixth Petroleum Geology Conference, Petroleum Geology Conferences Ltd. Geological Society, London, pp. 1095–1107.

Hunsdale, R., Taylor, R.N., Nesbitt, R.W., 1995. Characterisation and possible dating of fault seal in southern England. In: Underhill, J.R. (Convenor). The Development and Evolution of the Wessex Basin and Adjacent Areas. Petroleum Group Meeting 27–28 June 1995. Abstract volume, Geological Society, London, 2pp (unnumbered).

Kamerling, P., 1979. The geology and hydrocarbon habitat of the Bristol Channel Basin. Journal of Petroleum Geology 2, 75–93.

Kelly, P.G., Peacock, D.C.P., Sanderson, D.J., McGurk, A.C., 1999. Selective reverse-reactivation of normal faults and deformation around reverse-reactivated faults. Journal of Structural Geology 21, 493–509.

Lake, S.D., Karner, G.D., 1987. The structure and evolution of the Wessex Basin. Tectonophysics 137, 347–378.

Lloyd, A.J., Savage, R.J.G., Stride, A.H., Donovan, D.T., 1973. The geology of the Bristol Channel floor. Philosophical Transactions of the Royal Society of London 274A, 595–626.

Lowell, J.D., 1995. Mechanics of basin inversion from worldwide examples. In: Buchanan, J.G., Buchanan, P.G. (Eds.), Basin Inversion. Geological Society, London, Special Publication 88, pp. 39–57.

McClay, K.R., 1989. Analogue models of inversion tectonics. In: Cooper, M.A., Williams, G.D. (Eds.), Inversion Tectonics. Geological Society, London, Special Publication 44, pp. 41–59.

McClay, K.R., 1995. The geometrics and kinematics of inverted fault systems: a review of analogue model studies. In: Buchanan, J.G., Buchanan, P.G. (Eds.), Basin Inversion. Geological Society London Special Publication 88, pp. 97–118.

McClay, K.R., Dart, C.J., 1993. Field guide: Fault Tectonics of the North Somerset Coast. Fault Dynamics Project, Royal Holloway, University of London, Egham, Surrey.

McClay, K.R., Insley, M.W., Anderton, R., 1989. Inversion of the Kechika Trough, northeastern British Columbia, Canada. In: Cooper, M.A., Williams, G.D. (Eds.), Inversion Tectonics. Geological Society of London, Special Publication 44, pp. 235–257.

McGrath, A.G., Davison, I., 1995. Damage zone geometry around fault tips. Journal of Structural Geology 17, 1011–1024.

Menpes, R.J., Hillis, R.R., 1995. Quantification of Tertiary erosion in the Celtic Sea/South Western approaches. In: Buchanan, J.G., Buchanan, P.G. (Eds.), Basin Inversion. Geological Society, London, Special Publication 88, pp. 191–207.

Nemčok, M., Gayer, R., Miliorizos, M., 1995. Structural analysis of the inverted Bristol Channel Basin: implications for the geometry and timing of fracture porosity. In: Buchanan, J.G., Buchanan, P.G. (Eds.), Basin Inversion. Geological Society, London, Special Publication 88, pp. 355–392.

Owen, T.R., 1971. The structural evolution of the Bristol Channel. In: Ordinary General Meeting 13 May 1970. Proceeding of the Geologists Society, London 1664, pp. 289–294.

Peacock, D.C.P., Sanderson, D.J., 1991. Displacements, segment linkage and relay ramps in normal fault zones. Journal of Structural Geology 13, 721–733.

Peacock, D.C.P., Sanderson, D.J., 1994. Geometry and development of relay ramps in normal faults zones. Bulletin of the American Association of Petroleum Geologists 78, 147–165.

Peacock, D.C.P., Sanderson, D.J., 1996. Strike-slip relay ramps. Journal of Structural Geology 17, 1351–1360.

Petit, J.P., 1987. Criteria for the sense of movement on fault surfaces in brittle rocks. Journal of Structural Geology 9, 597–608.

Powell, C.M., 1987. Inversion tectonics in S.W. Dyfed. Proceedings of the Geologists' Association 98, pp. 193–203.

Ramsay, J.G., Huber, M.I., 1987. The Techniques of Modern Structural Geology, 2: Folds and Fractures. Academic Press, London.

Rawnsley, K.D., Peacock, D.C.P., Rives, T., Petit, J.-P., 1998. Joints in the Mesozoic sediments around the Bristol Channel Basin. Journal of Structural Geology 20, 1641–1661.

Sibson, R.H., 1995. Selective fault reactivation during basin inversion: potential for fluid redistribution through fault-valve action. In: Buchanan, J.G., Buchanan, P.G. (Eds.), Basin Inversion. Geological Society, London, Special Publication 88, pp. 3–19.

Smith, C., Hatton, I.R., 1998. Inversion tectonics in the Lyme Bay–West Dorset area of the Wessex Basin, UK. In: Underhill, J.R. (Ed.), Development, Evolution and Petroleum Geology of the Wessex Basin. Geological Society, London, Special Publication 133, pp. 267–281.

Tappin, D.R., Chadwick, R.A., Jackson, A.A., Wingfield, R.T.R., Smith, N.J.P., 1994. United Kingdom offshore regional report: the geology of Cardigan Bay and the Bristol Channel. HMSO for the British Geological Survey, London, 107pp.

Turner, J.P., Williams, G.A., 2004. Sedimentary basin inversion and intra-plate shortening. Earth Science Reviews 65, 37–304.

Walsh, J.J., Watterson, J., 1987. Distributions of cumulative displacement and seismic slip on a single normal fault surface. Journal of Structural Geology 9, 1039–1046.

Walsh, J.J., Watterson, J., 1990. New methods of fault projection for coalmine planning. Proceedings of the Yorkshire Geological Society 48, 209–219.

Welbon, A., 1988. The influence of intrabasinal faults on the development of a linked thrust system. Geologische Rundschau 77, 11–24.

Whittaker, A., 1972. The Watchet Fault—a post Liassic transcurrent reverse fault. Bulletin of the Geological Survey of Great Britain 41, 75–80.

Whittaker, A., 1975. A postulated post-Hercynian rift valley system in southern Britain. Geological Magazine 112, 137–149.

Whittaker, A., 1976. Notes on the Lias outlier near Selworthy, west Somerset. Proceedings of the Ussher Society 3, 355–359.

Whittaker, A., Green, G.W., 1983. Geology of the country around Weston-super-Mare. Memoir Geological Survey of Great Britain, sheet 279, with parts of sheets 263 and 295, 147pp.

Whittaker, A., Green G.W., Kelk, B., 1980. Weston-super-Mare sheet 279 and parts of 263 and 295. 1:50,000 series. Geological Survey of Great Britain.